Metabolic Engineering 20 (2013) 198–211

Contents lists available at ScienceDirect

Metabolic Engineering

journal homepage: www.elsevier.com/locate/ymben

Characterization of two geraniol synthases from *Valeriana officinalis* and *Lippia dulcis*: Similar activity but difference in subcellular localization

Lemeng Dong [a], Karel Miettinen [b], Miriam Goedbloed [a], Francel W.A. Verstappen [a], Alessandra Voster [c], Maarten A. Jongsma [c], Johan Memelink [b], Sander van der Krol [a], Harro J. Bouwmeester [a,*]

[a] Laboratory of Plant Physiology, Wageningen UR, P.O. Box 658, 6700 AR Wageningen, The Netherlands
[b] Institute of Biology, Sylvius Laboratory, Leiden university, P.O. Box 9505, 2300 RA Leiden, The Netherlands
[c] Plant Research International, Wageningen UR, P.O. Box 619, 6700 AP Wageningen, The Netherlands

ARTICLE INFO

Article history:
Received 30 January 2013
Received in revised form
17 June 2013
Accepted 9 September 2013
Available online 21 September 2013

Keywords:
Engineering
Subcellular localization
Geraniol synthase
Metabolic profiling
Enzyme assay

ABSTRACT

Two geraniol synthases (GES), from *Valeriana officinalis* (*VoGES*) and *Lippia dulcis* (*LdGES*), were isolated and were shown to have geraniol biosynthetic activity with K_m values of 32 μM and 51 μM for GPP, respectively, upon expression in *Escherichia coli*. The *in planta* enzymatic activity and sub-cellular localization of VoGES and LdGES were characterized in stable transformed tobacco and using transient expression in *Nicotiana benthamiana*. Transgenic tobacco expressing VoGES or LdGES accumulate geraniol, oxidized geraniol compounds like geranial, geranic acid and hexose conjugates of these compounds to similar levels. Geraniol emission of leaves was lower than that of flowers, which could be related to higher levels of competing geraniol-conjugating activities in leaves. GFP-fusions of the two GES proteins show that VoGES resides (as expected) predominantly in the plastids, while LdGES import into to the plastid is clearly impaired compared to that of VoGES, resulting in both cytosolic and plastidic localization. Geraniol production by VoGES and LdGES in *N. benthamiana* was nonetheless very similar. Expression of a truncated version of *VoGES* or *LdGES* (cytosolic targeting) resulted in the accumulation of 30% less geraniol glycosides than with the plastid targeted VoGES and LdGES, suggesting that the substrate geranyl diphosphate is readily available, both in the plastids as well as in the cytosol. The potential role of GES in the engineering of the TIA pathway in heterologous hosts is discussed.

1. Introduction

Plants are estimated to produce more than 500,000 secondary metabolites of various classes (isoprenoids, phenylpropanoids, alkaloids) (Hadacek, 2002). Of these, the isoprenoids represent the largest family based on their diverse structural features which relate to numerous biological activities. Isoprenoids have been shown to affect many physiological processes such as respiration, signal transduction, cell division, membrane architecture, photosynthesis, and growth. In addition, isoprenoids have ecological significance as they play an important role in the exchange of signals between plants and between plants and microorganisms or in defense against pathogens and herbivores. Also the applications of isoprenoids in foods, cosmetics and pharmaceutical drugs make specific terpenoids interesting commerical targets.

Although isoprenoids are extraordinarily diverse, they all originate from the condensation of the universal five-carbon precursors, isopentenyl diphosphate (IPP) and dimethyl allyl diphosphate (DMAPP). In higher plants, two independent pathways, located in separate intracellular compartments, are involved in the biosynthesis of IPP and DMAPP. In the cytosol, IPP is derived from the classic mevalonic acid (MVA) pathway that starts from acetyl-CoA (Porter and Spurgeon, 1981), whereas in plastids, IPP is formed from pyruvate and glyceraldehyde 3-phosphate via the methylerythritol phosphate (MEP or non-mevalonate) pathway (Eisenreich et al., 2001; Lichtenthaler, 1999). Cytosolic IPP and DMAPP are converted to farnesyl diphosphate (FPP, C15), which serves as a precursor of sesquiterpene and triterpene biosynthesis in the cytosol. In contrast, the plastidial pool of IPP/DMAPP is converted to geranyl diphosphate (GPP, C10) and geranylgeranyl diphosphate (GGPP, C20) which serve as precursors for monoterpenes, and diterpenes and tetraterpenes, respectively, in the plastid (Lange et al., 2001; McConkey et al., 2000; Tholl and Lee, 2011; Turner et al., 1999).

* Corresponding author.
E-mail address: harro.bouwmeester@wur.nl (H.J. Bouwmeester).

1096-7176/$ - see front matter © 2013 International Metabolic Engineering Society. Published by Elsevier Inc. All rights reserved.
http://dx.doi.org/10.1016/j.ymben.2013.09.002

Geraniol is an acyclic monoterpene alcohol that is synthesized in one step from GPP. Geraniol is a component of essential oils present in many fragrant plant species (Antonelli et al., 1997; Bakkali et al., 2008; Bayrak and Akgül, 1994; Sangwan et al., 2001; Yang et al., 2005). It has a rose-like odor and is commonly used in perfumes (Chen, 2006; Rastogi et al., 2003) and aromatic fragrance in wine (Herrero et al., 2008; Pedersen et al., 2003). Geraniol also has pharmaceutical properties, as it can inhibit the growth of human colon cancer cells (Carnesecchi et al., 2001) and interfere with membrane functions in *Candida albicans* and *Saccharomyces cerevisiae* (Bard et al., 1988). In some plant species geraniol is the precursor for terpenoid indole alkaloid (TIA) biosynthesis. For instance, in *Catharanthus roseus* the anticancer agents vinblastine and vincristine are synthesized from geraniol (monoterpene iridoid branch) and tryptophan (indole branch) in the TIA pathway.

Multiple approaches have been tested to increase TIA production. For example, overexpress gene 1-deoxy-D-xylulose synthase and geraniol-10-hydroxylase gene were shown to increase the flux towards vinblastine and vincristine in *C. roseus* hairy root (Peebles et al., 2011). Attempts to boost transcription of TIA biosynthetic genes in the hairy roots or suspension cells were only partially successful (Liu et al., 2011; Memelink and Gantet, 2007; Montiel et al., 2007). For example, ORCA3 is a jasmonate responsive transcription factor that promotes transcription of TIA biosynthesis genes (Vom Endt et al., 2007). However, when ORCA3 is overexpressed, also repressor activity is activated, which in the long term actually caused a decrease in several TIA metabolites in *C. roseus* (Peebles et al., 2009). Expression of the TIA pathway biosynthesis genes in a heterologous host may provide a way to overcome such feedback regulation problems.

The objective of the present study was the efficient production of the monoterpene geraniol as the first step in a larger program to rebuild the complete monoterpene iridoid branch of the TIA biosynthesis pathway in a heterologous host. To achieve this, a geraniol synthase (GES) was cloned from *V. officinalis* L. (Valerianananceae) (*VoGES*) and compared to the previously isolated *LdGES* from *L. dulcis* (Yang et al., 2011). Both proteins showed similar geraniol synthase activity *in vitro* and *in planta*. VoGES was subsequently used in a number of transient and stable metabolic engineering approaches to explore the possibility to reconstitute the monoterpene branch of TIA biosynthesis in tobacco.

2. Materials and methods

2.1. Cloning and sequence analysis of geraniol synthase gene

For the cloning of the geraniol synthase gene, *V. officinalis* L. (VoGES) total RNA was isolated from *V. officinalis* leaves using SV Total RNA Isolation System (Promega). Based on conserved domains of known geraniol synthases, the degenerate primers (forward primer 5′–GAYGARAAYGGIAARTTYAARGA–3′ and reverse primer 5′–CCRTAIGCRTCRAAIGTRTCRTC–3′) were designed to amplify partial cDNA fragment by reverse transcription PCR (RT-PCR). Full length sequences of the cDNAs were obtained by rapid amplification of cDNA ends (RACE).

Putative VoGES sequence was blasted against the GenBank ENTREZ database (NCBI Blast 2.2.23) (Altschul et al., 1997) and GES sequences were aligned using CLUSTALX 1.83 (Thompson et al., 1997) using standard settings. Prediction of the subcellular localization was from the targeting prediction programs PREDOTAR version 1.03 (http://urgi.versailles.inra.fr/predotar/) (Small et al., 2004) and TARGETP 1.1 Server (http://www.cbs.dtu.dk/services/TargetP/) (Emanuelsson et al., 2000).

2.2. Heterologous expression of VoGES and LdGES protein in E. coli

For the *in vitro* functional analysis of the putative geraniol synthase from *V. officinalis* and comparison with *LdGES*, the truncated cDNAs Δ*NVoGES* (bp 178-1785) and Δ*NLdGES* (bp 139-1755) were subcloned into the multiple cloning site of the expression vector pRSET A (Invitrogen) to yield constructs pRSET-ΔNVoGES and pRSET-ΔNLdGES. Primer sequences for PCR amplification and restriction sites for each primer are listed in Table S1. After full re-sequencing to check integrity, constructs were transformed into *E. coli* BL21 (DE3) (Invitrogen) and expression was induced by isopropyl β-D thiogalactopyranoside (IPTG) in transformed *E. coli* BL21 (DE3) cell cultures. The His-tagged proteins were isolated by passing through Ni-NTA Spin columns according to the manufacturers' recommendations (Qiagen). For quality analysis, the recombinant protein was confirmed with 12.5% (w/v) SDS-PAGE gel electrophoresis followed by Western blotting using mouse monoclonal anti-His horseradish peroxidase (HPR) conjugate antibodies (5Prime, http://www.5prime.com). Antibody binding was detected by incubation in 250 μM sodium luminol, 0.1 M Tris–HCl (pH 8.6), 3 mM H_2O_2, 67 μM *p*-coumaric acid and exposure to X-ray film.

An enzyme assay was carried out for functional characterization, using geranyl diphosphate (GPP) and farnesyl diphosphate (FPP) as substrates. Enzymatic assays were done in 0.5 ml reaction buffer containing 50 mM Tris–HCl, 1 mM $MgCl_2$, 0.1 mM $MnCl_2$, and 10, 20, 50 or 100 μM GPP (or 62.5 μM FPP) and 0.5 μg (VoGES) and 2 μg (LdGES) of purified enzyme. The reaction mixture was incubated at 32 °C for 5 min. For quantitative analysis citronellol was added to a concentration of 50 μM as an internal standard into the reaction tube after incubation. The reaction was stopped by adding 1 volume of hexane, mixing thoroughly by vortexing and keeping on ice for 10 min. The tubes were centrifuged at 4000*g* for 10 min, and the supernatant hexane phase was collected. The extraction was repeated with hexane (0.5 ml). Then the hexane phase was collected and dehydrated and then subjected to capillary gas chromatography–flame ionizing detector (GC–FID) and gas chromatography–mass spectrometry (GC–MS, supplementary method). For the latter, the hexane extract was separated on a Agilent GC 6890 series equipped with a DB-5 capillary column (30 m × 0.25 mm, film thickness of 0.25 μm) (J&W Scientific) using nitrogen as carrier gas at a flow rate of 1.2 ml min^{-1}. The separation conditions were: split mode 1: 5, injection volume 5 μl, injector temperature 230 °C, initial oven temperature 100 °C, then linear gradient to 140 °C at a rate of 10 °C min^{-1} followed by a linear gradient to 240 °C at a rate of 35 °C min^{-1}. Amounts of geraniol formed in enzyme assays were calculated from the resultant GC/FID integral using the relative response factor with respect to the citronellol internal standard. Lineweaver–Burk plots of VoGES and LdGES activity were used to obtain the K_m values for GPP.

2.3. VoGES and LdGES subcellular localization studies

For analysis of the subcellular targeting, the coding sequences of *EGFP* were fused to the N-terminus or C-terminus of full length *VoGES* and *LdGES*. In addition a truncated version of LdGES lacking the first 46 AA (Δ*NLdGES*: bp 139-1755) and a truncated version of VoGES lacking the first 56 AA (Δ*NVoGES*: bp 178-1785) was made using standard cloning techniques and the C-terminal coding sequence of these genes was fused in frame to that of GFP. The *VoGES–GFP*, *LdGES–GFP*, *GFP–VoGES*, *GFP–LdGES*, Δ*NVoGES–GFP* and Δ*NLdGES–GFP* were cloned into impact vector pIV2A 2.1 (www.pri.wur.nl/UK/products/ImpactVector/) under control of the CaMV 35S-promoter. In addition, the truncated versions of *VoGES* and *LdGES* were provided with a heterologous plastid import signal by cloning into impact vector pIV2A 2.4 which

carries an artificial plastid targeting signal (www.pri.wur.nl/UK/products/ImpactVector/) (Wong et al., 1992). The fusion constructs were sequenced to check integrity, before transferring the fusion cassettes to the binary vector pBIN+ (van Engelen et al., 1995) using LR recombination (Gateway technology) (Karimi et al., 2002). Primer sequences for PCR amplification and restriction sites for each primer are listed in Table S1. Finally, the binary expression constructs were transformed into *Agrobacterium tumefaciens* strain AGL0 (Lazo et al., 1991) which was used for transient expression in *N. benthamiana* as described below. Expression and localization were analyzed at different days post-agroinfiltration in small leaf samples ($\sim$0.5 cm^2 leaf material from at least three independent agro-infiltrated plants) by confocal laser scanning.

Microscopy using an Axiovert 200 M with a Zeiss LSM 5 Pa laser scanning microscope (Carl Zeiss) and a 20× (N.A. 0.5) Plan NeoFluar (Zeiss) or a 63× (N.A. 1.4 oil) Plan Apochromat (Zeiss) objective. Samples were excited with 1% of a 488 nm laser (emission from a 30 mW argon tube) for *EGFP* and chlorophyll excitation and green *EGFP* fluorescence and red chlorophyll fluorescence were collected using two emission filters. Band pass was set to 505–530 nm for *EGFP* fluorescence detection and long pass was set to >560 nm for chlorophyll autofluorescence detection. Images were exported from.lsm files to.tif files using Zeiss LSM image browser version 3.5 without further processing.

2.4. Tobacco stable plant transformation

The *VoGES* and *LdGES* full length cDNA sequences were subcloned into the binary expression vector pBIN+ using standard cloning techniques. In this vector *VoGES* and *LdGES* are under the control of the constitutive CaMV-d35S promoter and a nopaline synthase terminator. Both the 35S::*LdGES* and 35S::*VoGES* pBIN+ constructs were introduced into *A. tumefaciens* AGL0 and *in vitro* grown wild-type *Nicotiana tobacum* 'Samsun NN' was transformed using the leaf disc method as described (Horsch et al., 1985). Transformed shoots were selected on medium with 100 mg/l kanamycin. Primary transformed shoots were rooted on non-selective medium, checked by PCR for presence of the expression construct and positive T0 shoots were transferred to soil and grown until seed set. T1 plants were grown until seed set and from the T2 population five homozygous lines 35S::*LdGES* and three homozygous lines 35S::*VoGES* with single insert were selected.

2.5. Transient expression in N. benthamiana

A. tumefaciens infiltration (agro-infiltration) was performed according to the description of van Herpen et al. (2010). Briefly, *A. tumefaciens* was grown at 28 °C for 24 h in LB media with kanamycin (50 mg/l) and rifampicillin (34 mg/l). Cells were harvested by centrifugation for 20 min at 4000*g* and 20 °C and then resuspended in infiltration buffer containing 10 mM MES (2-(N-morpholino) ethanesulfonic acid, Duchefa Biochemie), 10 mM $MgCl_2$ and 100 μM acetosyringone (4′-hydroxy-3′, 5′-dimethoxyacetophenone, Sigma) to a final OD_{600} of $\sim$0.5, followed by incubation at room temperature under gentle shaking at 50 rpm for 150 min. In all experiments, *A. tumefaciens* harboring TBSV *p19* was included to maximize protein production by suppression of gene silencing (Voinnet et al., 2003). *A. tumefaciens* harboring constructs with *GFP–GES* or *GES* were infiltrated into leaves of five-week-old *N. benthamiana* plants by pressing a 1 mL syringe without metal needle against the abaxial side of the leaf and slowly injecting the bacterium suspension into the leaf. *N. benthamiana* plants were grown from seeds on soil in the greenhouse with a minimum of 16 h light. Day temperatures were approximately 28 °C, night temperatures 25 °C. After agro-infiltration the plants remained under the same greenhouse conditions until further analysis.

2.6. Volatile GC–MS analysis

For analysis of the production of volatiles by 35S::*LdGES* or 35S::*VoGES* tobacco seedling, T2 seeds were sterilized by chlorine bleach and placed on ½ MS (Duchefa, Netherlands) medium. Petri dishes with $\sim$50 seeds were incubated at 4 °C in the dark to ensure synchronous germination. Subsequently, petri dishes were transferred to growth cabinets with 16L/8D, 28 °C day, 25 °C night. After 2 weeks of growing, petri dishes were placed in 0.5 L glass jars, and volatiles were trapped for 5 h in the light using Tenax TA (20/35 mesh, Alltech, Breda, the Netherlands).

Headspace analysis of stable transformed *VoGES* tobacco was done using detached leaves and flowers. Before they were enclosed in 1 L glass jars with a Teflon-lined lid equipped with in- and outlet, detached leaves and flowers from tobacco plants at different development stages were placed into small glass bottles with water in them while different parts of flowers were placed on wet filter paper. A vacuum pump was used to draw air through the glass jar at approximately 100 ml min^{-1}, with the incoming air being purified through a glass cartridge (140 × 4 mm) containing 150 mg Tenax TA. At the outlet the volatiles emitted by the samples were trapped on a similar Tenax cartridge. After 5 h of trapping, the trapped volatiles were analyzed by Thermodesorption GC–MS using a thermal desorber (Unity, Markes International Limited) and a Trace GC Ultra (Thermo Electron Corporation) coupled with DSQ mass spectrometer (Thermo Electron Corporation). The tubes were first purged to remove water vapor and oxygen for 2 min at room temperature with helium flow of 50 ml min^{-1}. Then trapped volatiles were desorbed from the Tenax in the thermal desorber at 250 °C for 5 min. Volatiles were collected in an electrically cooled sorbent trap (Unity; Markes, Llantrisant) at 10 °C and injected into the analytical column (ZB-5MSI, 30 m × 0.25 mm ID, 1.0 μm-film thickness, Zebron, Phenomenex). The temperature program of the gas chromatograph started at 40 °C (3 min hold) and rose to 280 °C at 12 °C min^{-1}, with a hold at final temperature for 2 min. The mass spectrometer was set to scan from 45 to 300 m/z with a scan time of 5.4 scans s^{-1}. The helium flow was constant at 1.0 ml min^{-1}. Ionization potential was set at 70 eV. For quantification, a geraniol calibration curve was made with a series of standard solutions. The GC–MS results were analyzed using Xcalibur software (Thermo, Waltham). After headspace trapping for 5 h in the light, samples were frozen in liquid nitrogen and stored at −80 °C for further analysis.

2.7. GC–MS analysis of extracts

Volatile compounds accumulated in the plant material were extracted with dichloromethane (DCM) and measured by GC–MS as described above. Aliquots of 500 mg of frozen, powdered material in pre-cooled glass tubes were extracted twice with 3 ml DCM. Extracts were shortly vortexed, sonicated for 10 min, centrifuged for 10 min at 1200 g and filtered through a small glass column containing anhydrous Na_2SO_4. The eluent was concentrated extracts under a flow of nitrogen and 1 μl concentrated extracts were injected into the GC–MS column. The initial oven temperature was 45 °C for 1 min, and was increased to 300 °C at a rate of 10 °C min^{-1} and held for 5 min at 300 °C. For quantification of geraniol and oxidized geraniol products, standards of geraniol, geranial and geranic acid were injected at different concentrations to establish calibration curves. Each sample was spiked with 2 μg/μl *cis*-nerolidol as internal standard.

2.8. Analysis of geraniol-derived conjugates by LC–QTOF-MS and LTQ-Orbitrap-MS^n

Analysis of non-volatile compounds in transgenic tobacco extracts was done by liquid chromatography coupled to quadrupole

time-of-flight mass spectrometry (LC–QTOF-MS) (De Vos et al., 2007). Aliquots of 200 mg of frozen, powdered material were extracted with 0.6 ml 99.9% MeOH/0.133% formic acid in 1.5 ml Eppendorf vial. After short vortex and 15 min sonication, the extracts were centrifuged and filtered through 0.45 μm filters (SRP4, Sartorius, Germany) and 5 μl of the filtered extract was analyzed using a Waters Alliance 2795 HPLC connected to a QTOF Ultima V4.00.00 mass spectrometer (Waters, MS technologies, UK). Measurements were in negative ionization mode and leucine encephalin ([M − H]−=554.2620) was used as a lock mass for online mass calibration.

Acquisition of LC–MS data was performed under MassLynx 4.0 (Waters). MassLynx was used for visualization and manual processing of LC–PDA-MS data. Mass data were processed using metAlign version 1.0 (www.metalign.nl). Baseline and noise calculations were performed from scan number 70 to 2480. The maximum amplitude was set to 25,000 and peaks below three times the local noise were discarded. Multiple mass signals derived from the same compound were grouped using MSClust software (biotools.wurnet.nl) by multivariate mass spectra reconstruction (MMSR) (Tikunov et al., 2005). The selected mass intensities were normalized using log 2 transformation and standardized using range scaling, in which each value in a certain row, corresponding to the internal standard leucine encephalin, was divided by the intensity range observed for this row throughout all samples analyzed. Each row was then mean centered. Finally, the normalized and log-transformed data matrix was used for Principal Components Analysis implemented in GeneMath XT version 2.1.

Significance of differences in intensity of each aligned mass signal between samples was assessed using student *t*-test (level of significance set at 0.05). Masses showing significant difference were manually checked in MassLynx. Putative identification of metabolites was by determining the best fit elemental composition using C, H and O with the MassLynx software. For multiple possible molecular formulas (tolerance <5 ppm) the best matches were searched in the Dictionary of Natural Products and SciFinder databases for possible structures.

For further identification, selected compounds were targeted for fragmentation by an Accela HPLC tower connected to a LTQ Orbitrap hybrid mass spectrometer (Thermo Fisher Scientific). The instrument settings of HPLC and LTQ Orbitrap were used as described earlier (van der Hooft et al., 2011). The LTQ was programmed to use a window of 10D to isolate the mass of interest in MS1. The data-dependent fragmentation was set as follows: MS2 fragmentation of most intense ion in MS1; MS3 fragmentation of the 5 most intense fragment ions in MS2; MS4 fragmentation of the 5 most intense fragment ions in each MS3.

2.9. Glycosidase treatment

To quantify how much of the geraniol related products were modified by glycosylation, extracts were treated with glycosidase to release geraniol or geraniol related compounds. For this purpose, 200 mg infiltrated leaf material was ground in liquid nitrogen and extracted with 1 ml citrate phosphate buffer, pH 5.4. The extracts were prepared by brief vortexing and sonication for 15 min. 0.2 ml of Viscozyme L (Sigma) was added and overlaid with 1 ml of pentane to trap released volatiles and the samples were again vortexed. To trap released volatiles, 1 ml pentane was added on top of the extract. The mixture was incubated overnight at 37 °C, and subsequently extracted twice with 2 ml of pentane. Extracts were dehydrated using anhydrous Na_2SO_4 and concentrated to approximately 100 μl. An internal standard, *cis*-nerolidol was used to quantify the products. Samples were analyzed using GC–MS as described in Section 2.7.

3. Results

3.1. Functional characterization of geraniol synthase from V. officinalis and L. dulcis in vitro

The GES gene from *V. officinalis* (*VoGES*) encodes a protein which shares 37–67% identity with GES proteins from other plant species (Table 1, Fig. 1). Previous characterized GES gene from *L. dulcis* (*LdGES*) shares 63% identity with *VoGES*. The alignment shows that the Aspartate-rich DDxxD-motif for metal-dependent ionization of the prenyl diphosphate substrate (Bohlmann et al., 1998; Tarshis et al., 1996; Wendt and Schulz, 1998) is present in all GES sequences (Fig. 1). Both the VoGES and LdGES protein with N-terminal truncation were produced in *E. coli* (see Section 2) to compare the *in vitro* activity. Analysis of both recombinant protein by SDS-PAGE and Coomassie Brilliant Blue staining and immunoprobing with anti-His antibodies showed the presence of one major band (Fig. 2A). In the presence of GPP, both enzymes catalyzed the formation of the acyclic monoterpene alcohol geraniol, which was identified based on comparison with the retention time of authentic geraniol (Fig. 2) and the mass spectrum comparison with the NIST library (Fig. S2). Truncated VoGES and LdGES catalyzed the conversion of GPP to geraniol with a K_m value of 32 μM and 51 μM, respectively (Fig. S3). No product was detected when VoGES or LdGES were supplied with FPP (data not show).

3.2. Different subcellular localization of VoGES and LdGES

Monoterpene synthases are generally believed to be localized in the plastids, and also their precursor GPP is supposed to be produced in the plastids. Target P (Emanuelsson et al., 2000) predicts plastid targeting for all GES proteins except ObGES, which is predicted to be targeted to the mitochondria (Table 1). Transient expression of the GES–GFP fusion proteins in *N. benthamiana* leaves showed that for VoGES–GFP the fluorescence signal was located in the plastids (Fig. 3A). The fluorescence of VoGES–GFP

Table 1
Comparison of Geraniol synthase proteins from different plant species and their predicted location by Target P (http://www.cbs.dtu.dk/services/TargetP/).

Gene	Identities (%)							Full length	Predicted localization
	VoGES	LdGES	CrGES	ObGES	CtGES	PfGES	VvGES		
VoGES	100	63	67	59	42	37	57	594aa	Chloroplast
LdGES	63	100	66	68	39	36	54	584aa	Chloroplast
CrGES	67	66	100	63	42	36	57	589aa	Chloroplast
ObGES	59	68	63	100	41	35	50	567aa	Mitochondrion
CtGES	42	39	42	41	100	45	42	603aa	Chloroplast
PfGES	37	36	36	35	45	100	37	603aa	Chloroplast
VvGES	57	54	57	50	42	37	100	595aa	Chloroplast

TP: targeting peptide.

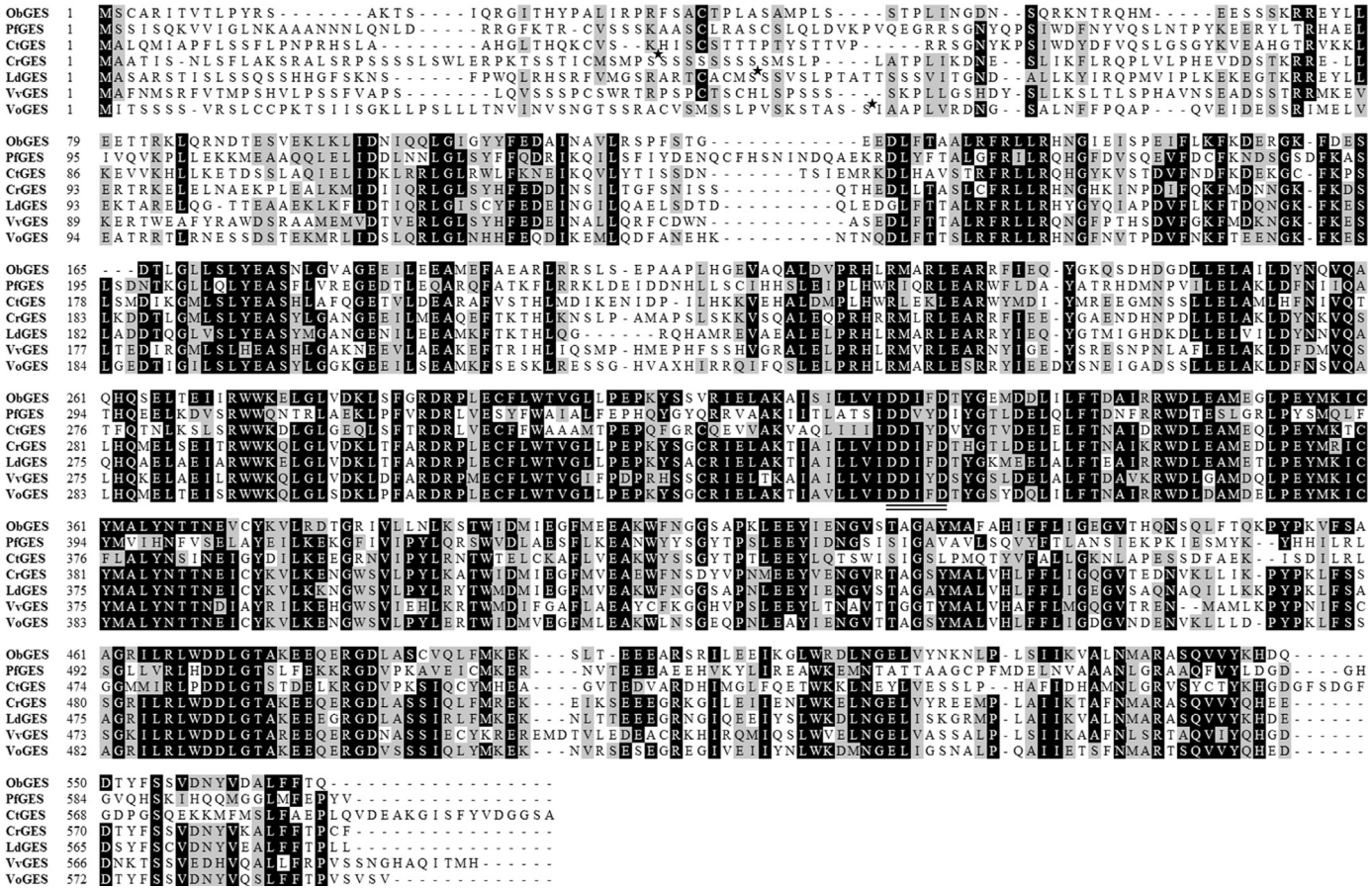

Fig. 1. Alignment of deduced amino acid sequences of ObGES (*Ocimum basilicum* geraniol synthase, AY362553), PfGES (*Perilla frutescens* geraniol synthase, DQ234300), CtGES (*Cinnamomum tenuipilum* geraniol synthase, AJ457070), CrGES (*Catharanthus roseus* geraniol synthase, AFD64744), LdGES (*Lippia dulcis* geraniol synthase, GU136162), VvGES (*Vitis vinifera* geraniol synthase, ADR74218), and VoGES (*Valeriana officinalis* geraniol synthase) using CLUSTALX 1.83 program. The metal ion-binding motif DDXXD is double underlined. The black star indicates the putative cleavage site of the targeting signal.

was also detected in the stromules that emanate from the plastids, which was most clearly observed in epidermal cells (Fig. 3B). However, for LdGES–GFP, the GFP fluorescence was observed in the cytosol and around the plastids (Fig. 3C). No stromule labeling was observed with LdGES–GFP in epidermal cells, confirming impaired import of LdGES into plastids and suggesting preferred localization in the cytosol. The cytosolic signal of GFP fluoresence can also be explained by instability of the LdGES–GFP fusion protein: if the GFP moiety is cleaved from the fusion protein in the cells, this would result in cytosolic localization. We therefore checked the integrity of the fusion proteins after transient expression in *N. benthamiana* on Western blots (Fig. S1). The western blot shows that the signal detected by anti-GFP is of the predicted size of the LdGES–GFP fusion protein (91 kD), indicating that the fluorescence signal is derived from the intact fusion protein, which for LdGES–GFP is located in mostly in the cytosol. For the N-terminal fusion proteins, both GFP–VoGES and GFP–LdGES (full length and truncated one) located (as expected) to the cytosol (Fig. 3D and E, result only show the GFP with full length). The fluorescence signal for LdGES–GFP and GFP–LdGES fusion proteins was consistently lower than that of VoGES–GFP, suggesting a lower stability for the LdGES protein.

3.3. *The different subcellular localization of VoGES and LdGES does not affect transient in planta activity*

GES is a monoterpene synthase which uses the substrate GPP, which is mostly synthesized in the plastidic MEP pathway. Because of the different subcellular location of VoGES and LdGES (Fig. 3), it was of interest to compare their *in planta* activity. For this purpose, the native VoGES, LdGES and the VoGES–GFP and LdGES–GFP fusion proteins were expressed transiently in *N. benthamiana* leaves. Ten days after agro-infiltration the plastidic (VoGES–GFP) and cytosolic (LdGES–GFP) targeting of the fusion protein was again confirmed by confocal fluorescence microscopy. No free geraniol was detected in the headspace of leaves expressing VoGES or LdGES and their GFP fusions when assayed at ten days post-agroinfiltration (not shown). However, previous experiments with expression of LdGES in maize had shown that the LdGES product geraniol may be converted by endogenous enzymes to geranial, geranic acid and other geraniol related products, which subsequently are sequestered as glycosylated compounds (Yang et al., 2011). Therefore, *N. benthamiana* leaves expressing the different constructs were extracted with citrate phosphate buffer and either mock treated or treated with Viscozyme, to release any glycosylated geraniol compounds. The released geraniol, geranial and geranic acid were trapped in the pentane overlay. Indeed, without glycosidase treatment, the levels of free geraniol and geraniol derivatives were below the level of detection by GC–MS in the citrate phosphate leaf extracts. In contrast, with Viscozyme treatment of the leaf samples, geraniol and the geraniol related compounds geranial, geranic acid, nerol, and neral were detected by GC–MS (Table 2). No geraniol or geraniol related products were detected after Viscozyme treatment of *N. benthamiana* leaves infiltrated with empty vector (Table 2). There was no significant difference in geraniol and the different geraniol derived products from free GES or the GES–GFP fusion proteins, indicating that the C-terminal fusion of GFP does not impair the GES activity.

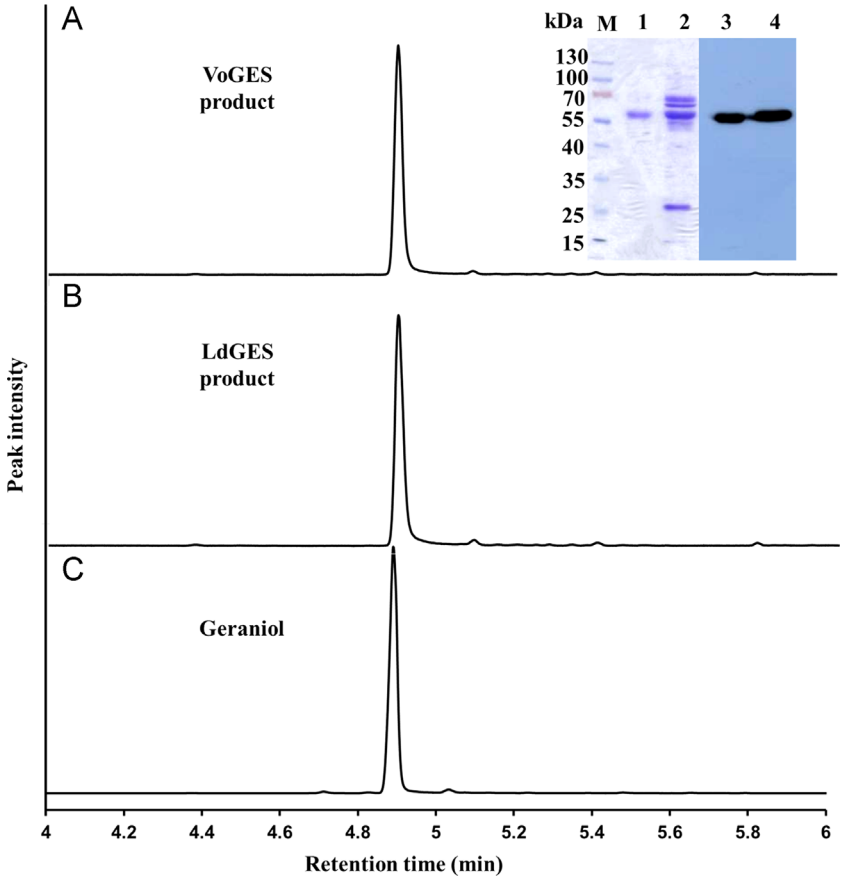

Fig. 2. GC–FID analysis of volatiles produced *in vitro* from GPP by ΔNVoGES (A) and ΔNLdGES (B) and of authentic geraniol (C). The insert in (A) shows the analysis of recombinant ΔNVoGES and ΔNLdGES protein. The protein was separated by SDS-PAGE and either stained with Coomassie Brilliant Blue (lane 1, ΔNVoGES; lane 2, ΔNLdGES) or visualized with Western blotting using anti-His antibodies (lane 3, ΔNVoGES; lane 4, ΔNLdGES).

Moreover, there was not much difference in GES related product accumulation for the full length VoGES and LdGES (Table 2). The presence of the products geranial, geranic acid, nerol, and neral indicates that geraniol was further converted to these products, likely by endogenous *N. benthamiana* enzymes.

To determine if geraniol production is possible from a cytosolic localized GES we tested an N-terminal truncated version of both *VoGES* and *LdGES* (Δ*NVoGES–GFP* and Δ*NLdGES–GFP*, respectively), which lack the plastid import signal. As expected, both these constructs showed cytosolic localization when expressed in *N. benthamiana* (Fig. 3F and G). In addition, we made expression constructs of the Δ*NLdGES* and Δ*NVoGES* with an N-terminal fusion to the same *A. thaliana* ribulose-1,5-bisphosphate carboxylase small subunit transit peptide (*pΔNLdGES* and *pΔNVoGES*, respectively) (Wong et al., 1992). The transient expression of Δ*NLdGES* and Δ*NVoGES* in *N. benthamiana* leaves resulted in similar levels of geraniol glycosides, but levels were about 30% lower than that produced by truncated genes fused to the heterologous plastid targeted signal (*pΔNLdGES* and *pΔNVoGES*) of the native *VoGES* and *LdGES* (Fig. 4).

3.4. Similar activity of VoGES and LdGES in stably transformed tobacco plants

Headspace analysis of stable transfomants of *N. tobacum* L. 'Samsun NN' showed no geraniol in the headspace of wild type plantlets, but plantlets transformed with either *VoGES* or *LdGES* expression constructs did emit geraniol into the headspace (Fig. 5A). Geraniol production differed between lines, but the production of geraniol was similar in the highest producer of *VoGES* and highest producer of *LdGES* transformants (Fig. 5B).

To analyze the production of non-volatile geraniol-derived products produced *in planta* in VoGES or LdGES transformed plants, the semipolar, non-volatile metabolites were analyzed by LC–QTOF-MS. PCA of reconstituted mass peaks (see materials and methods) shows clustering of the replicate groups and separation between WT and transgenic lines in the first component (49.7% of the variation; Fig. 5C). There was no separation between VoGES and LdGES, confirming that both GES proteins have very similar *in planta* activity, despite their different subcellular localization. Because of strong similarity in chemical profiles between the VoGES and LdGES lines, subsequently only VoGES18 was analyzed in more detail.

3.5. Different geraniol related compounds in flowers and leaves of transformed plants expressing GES

To determine free geraniol emission capacity of different parts of the plant, the headspace of leaves and flowers of different developmental stages was analyzed. Leaves were harvested from the plant at the onset of flowering. The headspace volatiles were collected for 5 h during the day. Analysis by GC–MS showed that the youngest leaves emit most geraniol and emission decreased in older leaves, while there was no significant difference between middle and old leaves (Fig. 6A). Analysis of flowers in different stages of development showed that emission was highest in freshly opened flowers (Fig. 6B). To understand which part of the flower contributes most to the geraniol emission, different parts of the tobacco flowers were isolated and separately analyzed

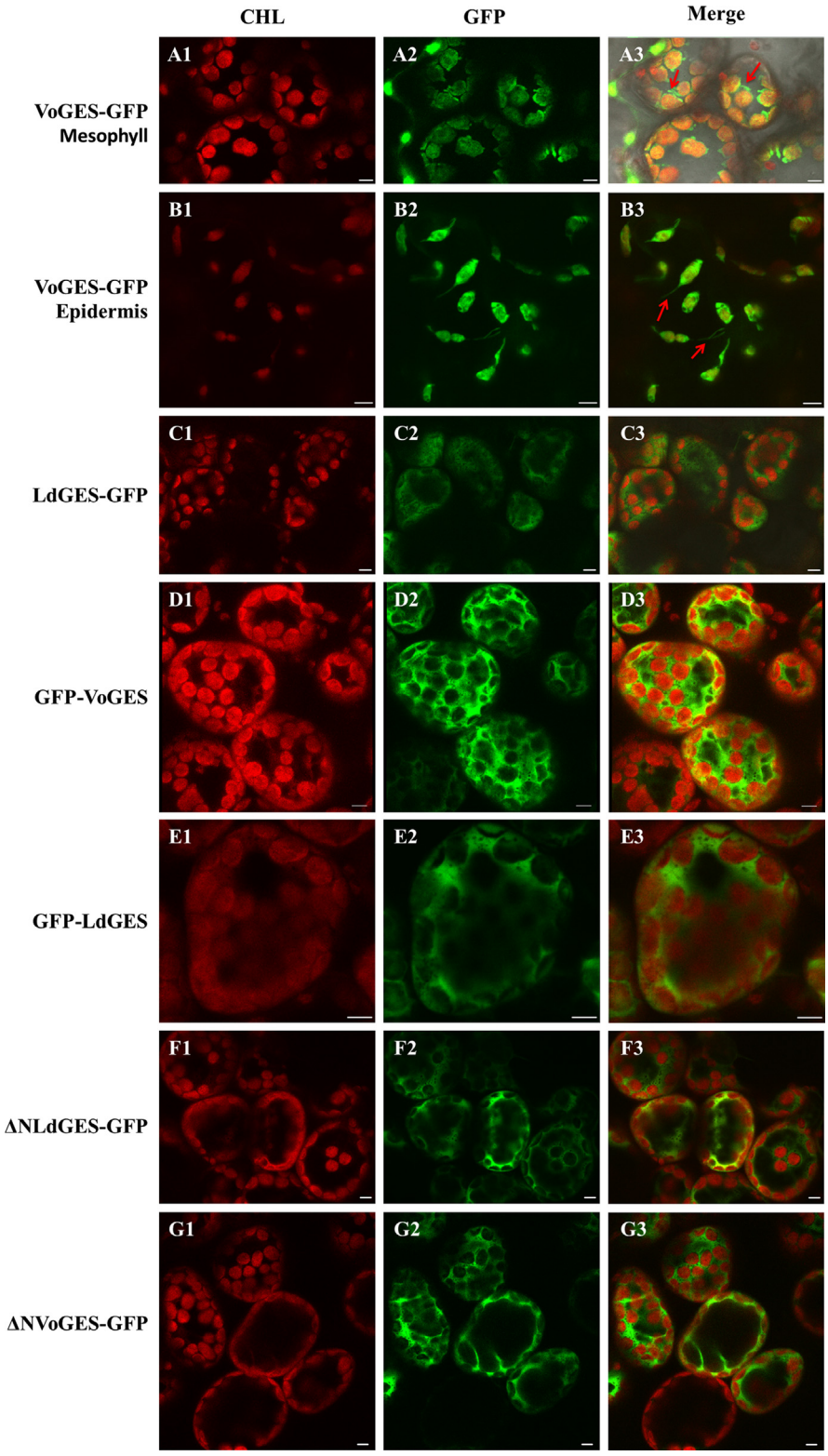

Fig. 3. Visualization of subcellular compartments of *N. benthamiana* cells using transient transformation with VoGES and LdGES fusion with epi-fluorescence GFP (e-GFP). A. VoGES–GFP (mesophyll cell), B. VoGES–GFP (epidermal cell), C. LdGES–GFP, D. GFP–VoGES, E. GFP–LdGES. F. ΔNLdGES–GFP, G. ΔNVoGES–GFP. CHL, chlorophyll autofluorescence (red), GFP, GFP fluorescence (green), Merge, merged green and red images. Arrows indicate stromules. Bar represents 5 μm. (For interpretation of the references to color in this figure legend, the reader is referred to the web version of this article.)

for headspace production. Fig. 6C shows that petal, sepal and ovary contribute almost equally to the geraniol in the total flower headspace. However, we noted that after dissection of the flower the production of geraniol increased almost 10-fold compared with the intact flower, possibly as a result of a wound induced increase in the flux through the MEP pathway (Bonaventure and Baldwin, 2010; Cordoba et al., 2009). Alternatively, it is possible that wounding results in induction of glycosidases that could liberate glycosidically bound geraniol (Edwards and Wratten, 1983; Hoagland, 1990).

Table 2
GC–MS quantification of geraniol and its derivatives in *N. benthamiana* leaves, *N. tobacum* leaves and flowers extracts.

	Geraniol		Geranial		Geranic acid		Nerol		Neral	
	Vis−	Vis+	Vis−	Vis+	Vis−	Vis+	Vis−	Vis+	Vis−	Vis+
N. benthamiana VoGES	nd	47.82 ± 5.14	nd	1.05 ± 0.11	nd	6.10 ± 0.27	nd	0.95 ± 0.95	nd	0.40 ± 0.06
N. benthamiana LdGES	nd	45.10 ± 10.24	nd	0.58 ± 0.29	nd	5.56 ± 1.15	nd	nd	nd	0.16 ± 0.08
N. benthamiana VoGES–GFP	nd	46.23 ± 3.85	nd	0.95 ± 0.18	nd	7.94 ± 1.25	nd	0.48 ± 0.08	nd	0.36 ± 0.06
N. benthamiana LdGES–GFP	nd	72.07 ± 17.55	nd	0.53 ± 0.38	nd	31.95 ± 10.51	nd	1.17 ± 0.48	nd	0.32 ± 0.16
N. benthamiana empty vector	nd	nd	nd	nd	nd	nd	nd	nd	nd	nd
N. tobacum VoGES leaf	4.25 ± 1.16	32.04 ± 9.53	nd	0.35 ± 0.05	nd	3.78 ± 0.22	nd	nd	nd	nd
N. tobacum VoGES flower	1.27 ± 0.21	6.39 ± 0.79	nd	0.27 ± 0.04	nd	5.79 ± 1.39	nd	nd	nd	nd
N. tobacum wild type	nd	nd	nd	nd	nd	nd	nd	nd	nd	nd

Results are the mean of 3 replicates ± standard deviation (μg/g fw). nd: not detected. Vis+: with Viscozyme treatment; Vis-: without Viscozyme treatment.

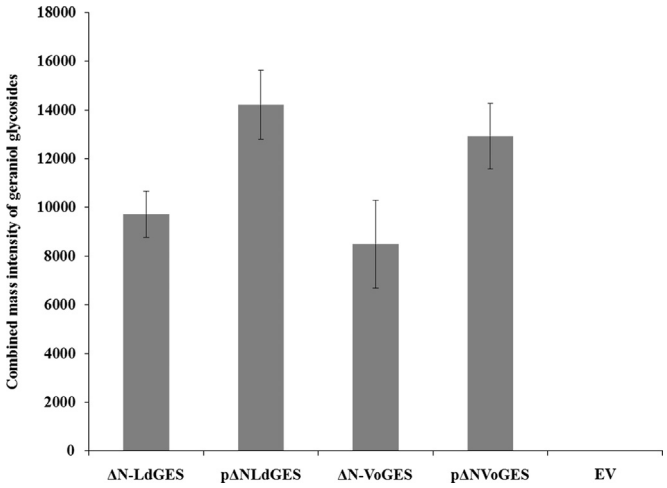

Fig. 4. Relative quantitative analysis of geraniol glycosides in agro-infiltrated *N. benthamiana* leaves with truncate (ΔN), artificial plastidic target (p) LdGES and VoGES and empty vector control (EV) by LC–MS. Bars represent the total mass intensity of all geraniol-derived glycosides (malonyl-hexosyl-geraniol, acetyl-hexosyl-hydroxy-dihydro-geranic acid, acetyl-dihexosyl-geraniol, hexosyl-carboxygeranic acid, hexosyl-hydroxy geraniol, pentosyl-hexosyl-geraniol and pentosyl-hexosyl-hydroxy-tetrahydro-geranic acid).

To determine the level of geraniol-derived glycosides in different tissues, leaves and flowers were treated with Viscozyme. Analysis of the released volatiles by GC–MS showed that without glycosidase treatment only geraniol is detected in the tissue extracts. Viscozyme treatment strongly increased geraniol production and now also geranial, and geranic acid were detected (Table 2). Combined, the level of glycosylated geraniol products in leaves (32.04 μg/g fw) were about 5-fold higher than in flowers (6.39 μg/g fw).

For analysis of the conjugated GES related products in the transformants the LC–MS chromatograms of WT and VoGES18 plants were compared and 19 compounds were identified with significantly higher signal in the transgenic line (Table 3). For identification of these putative geraniol-related products, the masses were targeted for fragmentation by LTQ Orbitrap MSn. According to the MSn spectra from 18 of the differential masses, the compounds are likely hexose, pentose and malonyl or acetyl conjugates of geraniol, hydroxy-geraniol, geranic acid, hydroxy-geranic acid and hydroxy-dihydro-geranic acid. One mass (709.3562), which is specific for sepal tissue could not be identified as a geraniol related product (Table 3). A malonylated hexosyl geranic acid conjugate was present in flower tissues but not in leaves, whereas a hexosyl hydroxyl-geranic acid conjugate was specific for leaves. Combined, the results suggest that the glycosylating activities for geraniol and geraniol derivatives are tissue-dependent. According to the mass intensity signal of the different glycoside conjugates in leaves, 89% were directly derived from geraniol, while 11% were apparently derived from geraniol after further modification to hydroxy-geraniol, geranic acid, hydroxy-geranic acid or hydroxy-dihydro-geranic acid (Fig. 7). In flowers, the proportion of geraniol and further modified products was slightly different from that in leaves in sepal, petal and ovary (Fig. 7), likely as a result of different endogenous enzyme activities in different tissues.

4. Discussion

4.1. Localization of VoGES in the plastids and LdGES mostly in the cytosol has no effect on in planta activity

In this study, we show that both VoGES and LdGES only produce the product geraniol *in vitro* as specific product from GPP (Fig. 2). Both VoGES and LdGES contain a putative plastid signal peptide (Table 1) and monoterpene synthases are generally believed to be active in the plastids (Bouvier et al., 2000; Dudareva et al., 2005; Turner et al., 1999). For instance, CrGES from *C. roseus* has been shown to be localized in the plastids (Simkin et al., 2012). Our localization experiments showed that VoGES directs the GFP protein to the plastids, as expected, and no cytosolic signal was observed from transient expression of *VoGES–GFP* in agroinfiltrated leaves of *N. benthamiana*, indicating that import into the plastids was not saturated. The plastidic localization of VoGES–GFP was also evident from GFP signal in the stromules extending from the plastids (Fig. 3A and B). In contrast, the signal of LdGES–GFP was mostly in the cytosol. Although some fluorescence in or around the plastids was observed, no LdGES–GFP signal was localized to the stromules of the plastids (Fig. 2C). Control experiments show that the cytosolic signal from LdGES–GFP does not result from cleavage of GFP from the fusion protein (Fig. S1). The GFP localization studies thus suggest a predominantly cytosolic localization of LdGES. Because product analysis (Table 2 and Fig. 5) shows that native VoGES and LdGES have similar activity *in planta*, this suggests that the substrate pool of GPP is not limiting for native LdGES in the cytosol. However, we also note that activity of the truncated VoGES and LdGES proteins (both localized to the cytosol) was only 30% of plastid localized VoGES and LdGES, suggesting that (although for these cytosolic GES proteins the GPP substrate is available) GPP is not as abundant available as in plastids. Indeed, it recently was shown that in tomato fruits cytosolic monoterpene biosynthesis can be supported by plastid-generated geranyl diphosphate substrate (Gutensohn et al., 2013). The higher activity of native (mostly) cytosolic LdGES and

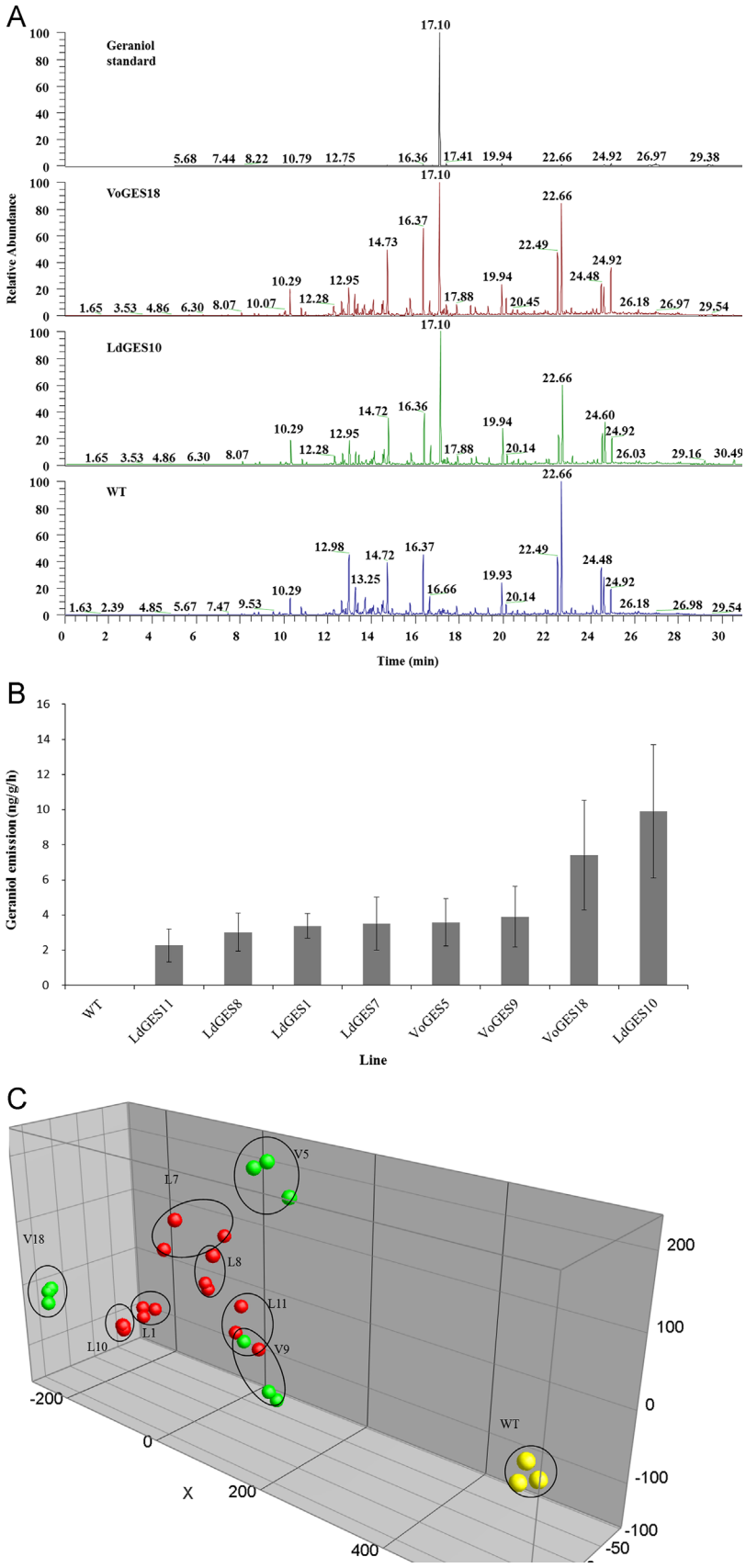

Fig. 5. GC–MS headspace analysis of volatiles and principal component analysis of non-volatiles on transgenic and wild type tobacco plantlets. A. GC chromatogram showing selected iron 69 of a geraniol standard, transgenic line VoGES18, LdGES10 and WT. Geraniol eluted at retention time 17.10 min. B. Geraniol concentration in the headspace of tobacco plantlets ($n=3$ groups ~50 plants). C. Principal component analysis of the LC–MS data on tobacco plantlets. PC1, PC2 and PC3 describe 49.7%, 21.5% and 15.3% of the total metabolic variation, respectively. V5, V9 and V18 indicate independent transgenic lines of VoGES; L1, L7, L8, L10 and L11 indicate independent transgenic lines of LdGES (three biological replicates of each line).

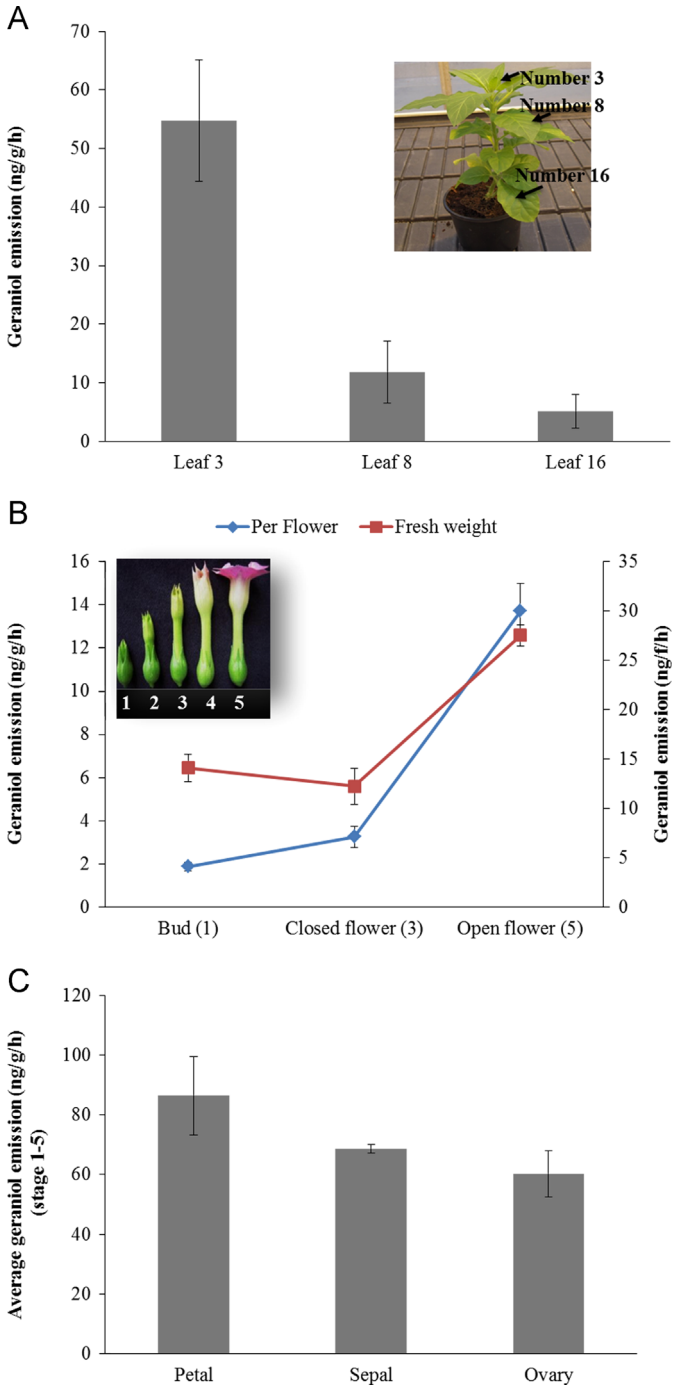

Fig. 6. Headspace analysis of different tissues of transgenic VoGES tobacco plants. A. Geraniol concentration of different developmental stage leaves. The numbers 3, 8 and 16 represent young (8 cm), middle (20 cm) and old (20 cm) age leaves, respectively. B. Geraniol emission of different developmental stage flowers. C. Geraniol emission of different parts of flowers.

truncated ΔNLdGES could be related to the partial plastidic localization of native LdGES.

4.2. Multiple oxidized and glycosylated forms of geraniol produced by endogenous enzymes

In our experiments approximately 11% of the produced geraniol was converted to the oxidized products geranial, hydroxy-geraniol, geranic acid, hydroxy-geranic acid and hydroxy-dihydro-geranic acid, which were mostly present as conjugates (Fig. 7, Table 3). These conversions of geraniol are likely catalyzed by endogenous tobacco enzymes. For examples, geranic acid is likely to be synthesized from geranial by an NAD+ dependent dehydrogenase (Boyer and Petersen, 1991; Campos-García, 2010; Davidovich-Rikanati et al., 2007; Lüddeke et al., 2012). Geranic acid was only present in glycosylated forms in the transgenic plants and not as the free form (Table 2). Because low levels of geranial were detected only after and not before de-glycosylation, presumably this product is formed from oxidation of geraniol during the de-glycosylation reaction.

4.3. Biotransformation of geraniol in different hosts

In this study, VoGES and LdGES were expressed in both a microbial, *E. coli*, and plant host (*N. benthamiana* and *N. tobacum*). With *E. coli* protein, we could only detect geraniol as product, while geraniol, geranial and geranic acid were observed in transiently expressing *N. benthamiana* as well as stable transformed *N. tobacum*. In addition, in *N. benthamiana* small amounts of nerol and neral were detected (Table 2). Previously it was shown that LdGES expressed in maize also results in geranyl acetate production in leaves (Yang et al., 2011), while this product was absent in *N. benthamiana* or tobacco plants expressing the same LdGES (this paper). This shows that different heterologous GES hosts metabolize the produced geraniol differently, and that especially plants tend to produce a wider spectrum of geraniol derivatives. Similar observation were made with expression of *Ocimum basilicum* geraniol synthase (ObGES) in yeast, *E. coli*, grape and tobacco (Fischer et al., 2012) and tomato (Davidovich-Rikanati et al., 2007). As expected, in all hosts the main product of ObGES was geraniol, but minor product (linalool, citronellol, nerol, α-terpineol…) formation differed between the heterologous hosts.

4.4. Different glycosylation patterns of geraniol products in different tissues and stages of development

Geraniol and geraniol derivatives accumulated in glycosylated form, some of which were further modified by endogenous malonyltransferases or acetyltransferases. The glycosides were mono-glycoside, di-glycosides and tri-glycosides. The hexoside, ubiquitous in nature, which can potentially be attached to geraniol is glucopyranoside, whereas the pentosides could be arabinofuranoside, arabinopyranoside, apiofuranoside, xylopyranoside or rhamnopyranoside (Genovés et al., 2005; Maicas and Mateo, 2005; Mateo and Jiménez, 2000). Presumably, the glycosylated geraniol products are sequestered in the vacuole (Wink, 2010; Winterhalter and Skouroumounis, 1997). The profile of glycosylated geraniol products differed between the agro-infiltrated *N. benthamiana* leaves and leaves of the stable transformed tobacco plants (Table 2). The glycosylation profile also differed between tissues and developmental stages within the same plant (Table 3). For instance, in the mature leaves of stable transformed tobacco plants expressing GES, the acetylated and malonylated glycosides of geraniol are ~5-fold higher than in seedlings (data not shown), suggesting that acelylation and malonylation are induced later during development. In total, the bioconversion by endogenous enzyme activities distributed the product of VoGES, geraniol, over at least 19 different compounds. Clearly, for effective reconstruction of a multiple step terpene biosynthesis pathway, such diversion of products needs to be avoided in order to raise the desired product yield. The use of different promoters, driving expression in tissues more specialized for the production and/or storage of terpenoids, could be one way to achieve this.

Table 3
LC–QTOF-MS and LTQ Qrbitrap Ms(n) analysis of non-volatile compounds significant difference between transgenic and WT plant.

Retention time	Observed mass	Putative identity	Calculated mass	ΔMass (ppm)	Elemental formula	MS(n) fragment	Tissue
24.04	345.1563	Hexosyl-hydroxy-geranic acid	345.1555	2.35	$C_{16}H_{25}O_8$	131, 143, 149, 161, 167, 179, 183, 206, 219, 261, 282, 299, 307, 327, 331	L
30.95	435.1862	Acetyl-hexosyl-hydroxy-dihydro-geranic acid (formic acid adduct)	435.1866	−0.92	$C_{19}H_{31}O_{11}$	157, 185, 205, 231, 249, 267, 291, 309, 315, 355, 375, 389, 417	L, S, P, O
32.98	435.1869	Acetyl-hexosyl-hydroxy-dihydro-geranic acid (formic acid adduct)	435.1866	0.69	$C_{19}H_{31}O_{11}$	131, 157, 185, 205, 231, 249, 267, 291, 309, 359, 373, 391, 417	L, S, P, O
40.20	447.2242	Pentosyl-hexosyl-geraniol	447.2235	1.52	$C_{21}H_{35}O_{10}$	131, 143, 149, 161, 179, 191, 233, 251, 293, 311, 315, 375, 401, 430	L, S, P, O
39.88	447.2243	Pentosyl-hexosyl-geraniol	447.2235	1.87	$C_{21}H_{35}O_{10}$	131, 143, 149, 161, 179, 191, 221, 239, 251, 275, 281, 293, 311, 315	L, S, P, O
39.17	447.2245	Pentosyl-hexosyl-geraniol	447.2235	2.28	$C_{21}H_{35}O_{10}$	131, 143, 149, 161, 179, 191, 217, 221, 233, 251, 281, 293, 311, 347, 420	L, S, P, O
38.45	461.2036	Pentosyl-hexosyl-geranic acid	461.2023	2.82	$C_{21}H_{33}O_{11}$	149, 191, 221, 239, 279, 293, 311, 339, 373, 389	L, S, P, O
42.41	461.2393	Deoxyhexosyl-hexosyl-geraniol	461.2392	0.21	$C_{22}H_{37}O_{10}$	161, 179, 213, 267, 295, 307, 323, 373, 385, 397, 415, 447	L, S, P, O
23.54	463.2178	Pentosyl-hexosyl-hydroxy-geraniol	463.2185	−1.40	$C_{21}H_{35}O_{11}$	143,149, 161, 191, 221, 251, 275, 293, 311, 331, 349, 387, 425	L, S
36.50	477.2335	Dihexosyl-geraniol	477.2331	0.75	$C_{22}H_{37}O_{11}$	161, 179, 221, 251, 281, 307, 323, 341, 361, 421, 449	L, S, P, O
25.37	611.2547	Dipentosyl-hexosyl-hydroxy-dihydro-geranic acid	611.2551	−0.65	$C_{26}H_{43}O_{16}$	149, 161, 191, 221, 251, 281, 293, 317, 347, 395, 429, 441, 461, 479	L, S, P
24.95	611.2560	Dipentosyl-hexosyl-hydroxy-dihydro-geranic acid	611.2551	1.47	$C_{26}H_{43}O_{16}$	149, 185, 221, 251, 275, 293, 311, 333, 360, 377, 435, 449, 461, 479	L, S, P
44.84	489.2329	Acetyl-pentosyl-hexosyl-geraniol	489.2336	−1.43	$C_{23}H_{37}O_{11}$	131, 149, 161, 191, 203, 233, 315, 327, 335, 367, 447, 463	L, S, P, O
47.39	503.2486	Acetyl-deoxyhexose-hexose-geraniol	503.2492	−1.19	$C_{24}H_{39}O_{11}$	143, 161, 203, 247, 307, 329, 443, 461, 477	L, S, P, O
37.06	579.2661	Dipentosyl-hexosyl-geraniol	579.2653	1.40	$C_{26}H_{43}O_{14}$	233, 293, 352, 372, 401, 425, 463, 493, 511, 567	L, S, P, O
34.30	609.2729	Pentosyl-dihexosyl-geraniol	609.2753	−3.94	$C_{27}H_{45}O_{15}$	191, 242, 267, 299, 315, 355, 387, 413, 447, 455, 475, 499, 537, 571	L, S, P, O
34.08	709.3562	Unknown 1	709.3588	−3.67	$C_{40}H_{53}O_{11}$	161, 173, 399, 445, 449, 467, 495, 541, 583, 609, 663, 699	S
47.95	803.3712	Malonyl-hexosyl-geraniol (dimer)	803.3701	1.31	$C_{38}H_{59}O_{18}$	131, 149, 161, 221, 329, 357, 401, 450, 501, 597, 643, 717	L, S, P
48.72	831.3299	Malonyl-hexosyl-geranic acid (dimer)	831.3287	1.44	$C_{38}H_{55}O_{20}$	161, 167, 191, 265, 307, 349, 371, 415	S, P, O

Δmass (ppm), deviation between the observed mass and calculated mass in ppm. L, S, P, O, leaf, sepal, petal, ovary.

4.5. No pleiotropic effects of GES overexpression

Introduction of GES into tobacco could potentially result in competition for the substrate GPP with other monoterpene synthases or result in depletion of the substrates isopentenyl diphosphate and dimethylallyl diphosphate which are important for the formation of other terpenes, carotenoids and gibberellins, and this could have a dramatic effect on the plant phenotype (Aharoni et al., 2003; Davidovich-Rikanati et al., 2007). However, no leaf or flower phenotype was observed in our stable transformed tobacco plants expressing VoGES or LdGES, despite high transgenic product levels suggesting that sufficient GPP is available in both leaves and flowers. Also, in the LC–MS and GC–MS analysis of transgenic plants or after transient expression of GES genes in *N. benthamiana*, only new products were detected but no obvious reduction in endogenous products, which suggests there is indeed no competition for substrate.

In the selected transgenic lines no pleiotropic effect of GES overexpression was observed. We cannot exclude that in the regeneration of stable transformed tobacco plants with 35S-VoGES or 35S-LdGES a selection occurred against very high GES expression, resulting in either toxic levels of geraniol or creating a drain of GPP required for other processes. Boosting of the GES production in the stable transformed tobacco plants (*e.g.* by combining with GPPS overexpression) could result in toxic effects of geraniol, but these effects may be eliminated by simultaneous co-expression with P450 enzymes which convert geraniol to less reactive intermediates/end products and/or by using tissue-specific promoters to drive geraniol production in tissues more specialized for terpene production and storage (for example trichomes).

4.6. Higher fluxes through geraniol sequestration than through geraniol emission

We note that emission of geraniol in stable transformed tobacco plants changed during development. For instance, in young seedlings emission was ~8 ng/g h, while in mature plants emission by leaves declined from young to old leaves from 55 to 5 ng/g h (Figs. 5 and 6). In flowers of stable transformants emission of geraniol increased until flowers were fully open from 12 to 28 ng/g h (Fig. 6). Based on the average headspace emission, the loss of geraniol from leaves would be ~17 μg/g month and from flowers ~13 μg/g month, while 37 μg/g fw of geraniol (derived) products (determined by de-glycosylation) are stored in 1 month old tobacco leaves (Table 2). *N. benthamiana* leaves at four days post-agroinfiltration show an average emission rate of 0.13 ng/g h (not shown), while no geraniol was emitted into the headspace ten days post-agro-infiltration (data not shown). This might suggest that after ten days not only has the T-DNA with the expression construct degraded, but that also the GES protein is no longer active in the cells, indicating a relatively high turn-over of terpene synthase protein.

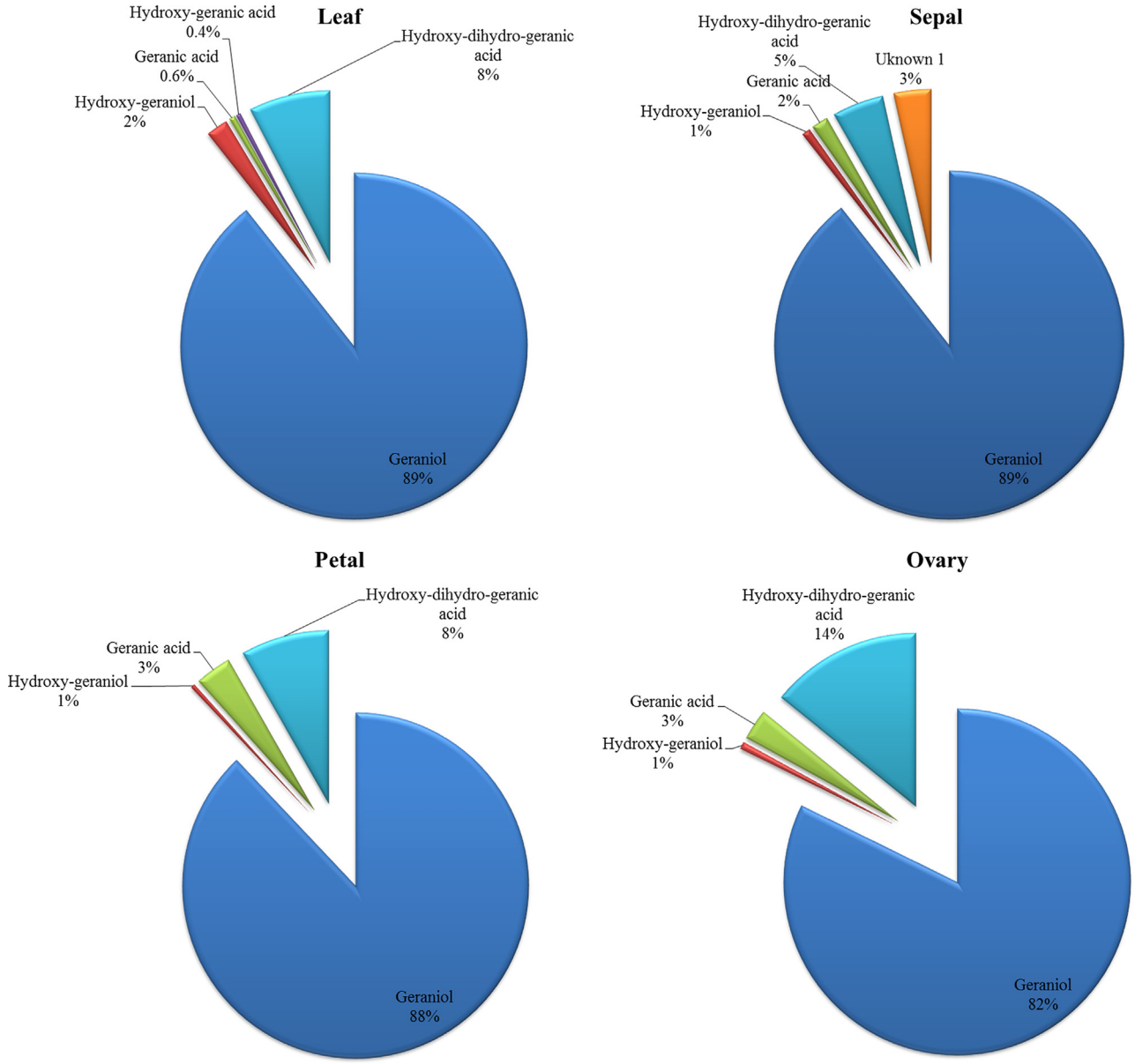

Fig. 7. Components of geraniol related aglycons based on mass intensity of putative glycosides in VoGES tobacco leaves and flowers.

Assuming that (1) effective expression in transient assays is from day 4 to 7 and that (2) geraniol production is at least 0.13 ng/g h in *N. benthamiana* leaves and that (3) flux through the pathway is 24 h/day (which may not be the case if precursors are preferably produced in the light (Aharoni et al., 2003)), the cumulative production of emitted geraniol over 4 days of transient expression would be ~0.012 μg/g fw. However, at ten days post agroinfiltration, the combined level of accumulated geraniol (derived) products (determined by de-glycosylation) was around 56 μg/g fw (Table 2).

Assuming that geraniol derived products in *N. benthamiana* accumulate during four days of continuous activity, this suggests a geraniol production of ~0.58 μg/g h fw. Total level of geraniol derived products in the stable transformants is ~37 μg/g fw and that is produced in 1 month, the geraniol production rate of stable transformants in tobacco is only 0.05 μg/g h fw. The high production in the transient assay is most likely due to an extremely high gene dosage number of the infiltrated GES expression construct compared to the low copy number in stable transformants. At present it is not clear why the high GES activity in the transient expression assay is not matched by a higher emission of geraniol, but one explanation may be that the conjugation capacity of infiltrated *N. benthamiana* leaves is highly efficient.

4.7. Towards a monoterpene iridoid pathway in heterologous plants

Expression of GES in tobacco is the first step in a larger effort to introduce the terpene indole alkaloid (TIA) biosynthesis into tobacco plants, consisting of a monoterpene iridoid branch and an indole branch (Mahroug et al., 2007; Simkin et al., 2012). The second step of this pathway is the conversion of geraniol to 10-hydroxy-geraniol by geraniol 10-hydroxylase (G10H), but (as described above) this conversion may already take place by endogenous tobacco enzymes (Table 3). We are currently testing whether co-expression of VoGES with a G10H can effectively compete for the endogenous unwanted oxidation and glycosylation of the primary product geraniol. In the context of multiple-step monoterpene pathway reconstruction in heterologous plant

hosts, elimination of the conversion by endogenous enzyme activities may become an important target for efficient channeling towards the desired product(s).

Acknowledgments

This research was funded by the European Community's Framework VII Program FP7/2007-2013 to the SMARTCELL project KBBE-2007-3-1-01. Lemeng Dong was supported by a PhD fellowship from China Scholarship Council. We thank Bert Schipper and Ric de Vos for their help with LC–MS analysis.

Appendix A. Supporting information

Supplementary data associated with this article can be found in the online version at http://dx.doi.org/10.1016/j.ymben.2013.09.002.

References

Aharoni, A., Giri, A.P., Deuerlein, S., Griepink, F., de Kogel, W.J., Verstappen, F.W.A., Verhoeven, H.A., Jongsma, M.A., Schwab, W., Bouwmeester, H.J., 2003. Terpenoid metabolism in wild-type and transgenic Arabidopsis plants. Plant Cell 15, 2866–2884.

Altschul, S., Madden, T., Schaffer, A., Zhang, J., Zhang, Z., Miller, W., Lipman, D., 1997. Gapped BLAST and PSI-BLAST: a new generation of protein database search programs. Nucleic Acids Res. 25, 3389–3402.

Antonelli, A., Fabbri, C., Giorgioni, M.E., Bazzocchi, R., 1997. Characterization of 24 old garden roses from their volatile compositions. J. Agric. Food Chem. 45, 4435–4439.

Bakkali, F., Averbeck, S., Averbeck, D., Idaomar, M., 2008. Biological effects of essential oils—a review. Food Chem. Toxicol. 46, 446–475.

Bard, M., Albrecht, M.R., Gupta, N., Guynn, C.J., Stillwell, W., 1988. Geraniol interferes with membrane functions in strains of *Candida* and *Saccharomyces*. Lipids 23, 534–538.

Bayrak, A., Akgül, A., 1994. Volatile oil composition of Turkish rose (*Rosa damascena*). J. Sci. Food Agric. 64, 441–448.

Bohlmann, J., Meyer-Gauen, G., Croteau, R., 1998. Plant terpenoid synthases: molecular biology and phylogenetic analysis. Proc. Natl. Acad. Sci. USA 95, 4126–4133.

Bonaventure, G., Baldwin, I.T., 2010. Transduction of wound and herbivory signals in plastids. Commun. Integr. Biol 3, 313–317.

Bouvier, F., Suire, C., d'Harlingue, A., Backhaus, R.A., Camara, B., 2000. Molecular cloning of geranyl diphosphate synthase and compartmentation of monoterpene synthesis in plant cells. Plant J. 24, 241–252.

Boyer, C.S., Petersen, D.R., 1991. The metabolism of 3, 7-dimethyl-2, 6-octadienal (citral) in rat hepatic mitochondrial and cytosolic fractions. Interactions with aldehyde and alcohol dehydrogenases. Drug Metab. Dispos. 19, 81–86.

Campos-García, J., 2010. Metabolism of acyclic terpenes by *Pseudomonas*. Pseudomonas, 235–253.

Carnesecchi, S., Schneider, Y., Ceraline, J., Duranton, B., Gosse, F., Seiler, N., Raul, F., 2001. Geraniol, a component of plant essential oils, inhibits growth and polyamine biosynthesis in human colon cancer cells. J. Pharmacol. Exp. Ther. 298, 197–200.

Chen, Y., 2006. Quantification of perfume compounds in shampoo using solid phase microextraction. Flavour Fragr. J. 21, 822–832.

Cordoba, E., Salmi, M., León, P., 2009. Unravelling the regulatory mechanisms that modulate the MEP pathway in higher plants. J. Exp. Bot. 60, 2933–2943.

Davidovich-Rikanati, R., Sitrit, Y., Tadmor, Y., Iijima, Y., Bilenko, N., Bar, E., Carmona, B., Fallik, E., Dudai, N., Simon, J.E., Pichersky, E., Lewinsohn, E., 2007. Enrichment of tomato flavor by diversion of the early plastidial terpenoid pathway. Nat. Biotechnol. 25, 899–901.

De Vos, R.C.H., Moco, S., Lommen, A., Keurentjes, J.J.B., Bino, R.J., Hall, R.D., 2007. Untargeted large-scale plant metabolomics using liquid chromatography coupled to mass spectrometry. Nat. Protoc. 2, 778–791.

Dudareva, N., Andersson, S., Orlova, I., Gatto, N., Reichelt, M., Rhodes, D., Boland, W., Gershenzon, J., 2005. The nonmevalonate pathway supports both monoterpene and sesquiterpene formation in snapdragon flowers. Proc. Natl. Acad. Sci. USA 102, 933–938.

Edwards, P., Wratten, S., 1983. Wound induced defences in plants and their consequences for patterns of insect grazing. Oecologia 59, 88–93.

Eisenreich, W., Rohdich, F., Bacher, A., 2001. Deoxyxylulose phosphate pathway to terpenoids. Trends Plant Sci. 6, 78–84.

Emanuelsson, O., Nielsen, H., Brunak, S., von Heijne, G., 2000. Predicting subcellular localization of proteins based on their N-terminal amino acid sequence. J. Mol. Biol. 300, 1005–1016.

Fischer, M.J., Meyer, S., Claudel, P., Perrin, M., Ginglinger, J.F., Gertz, C., Masson, J.E., Werck-Reinhardt, D., Hugueney, P., Karst, F., 2012. Specificity of *Ocimum basilicum* geraniol synthase modified by its expression in different heterologous systems. J. Biotechnol. 163, 24–29.

Genovés, S., Gil, J.V., Vallés, S., Casas, J.A., Manzanares, P., 2005. Assessment of the aromatic potential of palomino fino grape must using glycosidases. Am. J. Enol. Vitic. 56, 188–191.

Gutensohn, M., Orlova, I., Nguyen, T.T., Davidovich-Rikanati, R., Ferruzzi, M.G., Sitrit, Y., Lewinsohn, E., Pichersky, E., Dudareva, N., 2013. Cytosolic monoterpene biosynthesis is supported by plastid-generated geranyl diphosphate substrate in transgenic tomato fruits. Plant J 75, 351–363.

Hadacek, F., 2002. Secondary metabolites as plant traits: current assessment and future perspectives. Crit. Rev. Plant Sci. 21, 273–322.

Herrero, Ó., Ramón, D., Orejas, M., 2008. Engineering the *Saccharomyces cerevisiae* isoprenoid pathway for *de novo* production of aromatic monoterpenes in wine. Metab. Eng. 10, 78–86.

Hoagland, R.E., 1990. Biochemical responses of plants to pathogens. In: Hoagland, R.E. (Ed.), Microbes and Microbial Products as Herbi-cides American Chemical Society Symposium Series no. 439. ACS Books, Washington, DC, pp. 87–113.

Horsch, R., Fry, J., Hoffmann, N., Eichholtz, D., Rogers, S., Fraley, R., 1985. A simple and general method for transferring genes into plants. Science 227, 1229–1231.

Karimi, M., Inzé, D., Depicker, A., 2002. GATEWAY™ vectors for *Agrobacterium*-mediated plant transformation. Trends Plant Sci. 7, 193–195.

Lange, B.M., Ketchum, R.E.B., Croteau, R.B., 2001. Isoprenoid biosynthesis. Metabolite profiling of peppermint oil gland secretory cells and application to herbicide target analysis. Plant Physiol. 127, 305–314.

Lazo, G.R., Stein, P.A., Ludwig, R.A., 1991. A DNA transformation-competent *Arabidopsis* genomic library in *Agrobacterium*. Nat. Biotechnol. 9, 963–967.

Lichtenthaler, H.K., 1999. The 1-deoxy-D-xylulose-5-phosphate pathway of isoprenoid biosynthesis in plants. Annu. Rev. Plant Biol. 50, 47–65.

Liu, D.H., Ren, W.W., Cui, L.J., Zhang, L.D., Sun, X.F., Tang, K.X., 2011. Enhanced accumulation of catharanthine and vindoline in *Catharanthus roseus* hairy roots by overexpression of transcriptional factor ORCA2. Afr. J. Biotechnol. 10, 3260–3268.

Lüddeke, F., Wülfing, A., Timke, M., Germer, F., Weber, J., Dikfidan, A., Rahnfeld, T., Linder, D., Meyerdierks, A., Harder, J., 2012. Geraniol and geranial dehydrogenases induced in anaerobic monoterpene degradation by *Castellaniella defragrans*. Appl. Environ. Microbiol. 78, 2128–2136.

Mahroug, S., Burlat, V., St-Pierre, B., 2007. Cellular and sub-cellular organisation of the monoterpenoid indole alkaloid pathway in *Catharanthus roseus*. Phytochem. Rev. 6, 363–381.

Maicas, S., Mateo, J.J., 2005. Hydrolysis of terpenyl glycosides in grape juice and other fruit juices: a review. Appl. Microbiol. Biotechnol. 67, 322–335.

Mateo, J., Jiménez, M., 2000. Monoterpenes in grape juice and wines. J. Chromatogr. A 881, 557–567.

McConkey, M.E., Gershenzon, J., Croteau, R.B., 2000. Developmental regulation of monoterpene biosynthesis in the glandular trichomes of peppermint. Plant Physiol. 122, 215–224.

Memelink, J., Gantet, P., 2007. Transcription factors involved in terpenoid indole alkaloid biosynthesis in *Catharanthus roseus*. Phytochem. Rev. 6, 353–362.

Montiel, G., Breton, C., Thiersault, M., Burlat, V., Jay-Allemand, C., Gantet, P., 2007. Transcription factor Agamous-like 12 from *Arabidopsis* promotes tissue-like organization and alkaloid biosynthesis in *Catharanthus roseus* suspension cells. Metab. Eng. 9, 125–132.

Pedersen, D.S., Capone, D.L., Skouroumounis, G.K., Pollnitz, A.P., Sefton, M.A., 2003. Quantitative analysis of geraniol, nerol, linalool, and α-terpineol in wine. Anal. Bioanal. Chem. 375, 517–522.

Peebles, C.A., Hughes, E.H., Shanks, J.V., San, K.Y., 2009. Transcriptional response of the terpenoid indole alkaloid pathway to the overexpression of ORCA3 along with jasmonic acid elicitation of *Catharanthus roseus* hairy roots over time. Metab. Eng. 11, 76–86.

Peebles, C.A., Sander, G.W., Hughes, E.H., Peacock, R., Shanks, J.V., San, K.Y., 2011. The expression of 1-deoxy-D-xylulose synthase and geraniol-10-hydroxylase or anthranilate synthase increases terpenoid indole alkaloid accumulation in *Catharanthus roseus* hairy roots. Metab. Eng. 13, 234–240.

Porter, J.W., Spurgeon, S.L., 1981. In: Porter, J.W., Spurgeon, S.L. (Eds.), Introduction: Biosynthesis of Isoprenoid Compounds. John Wiley and Sons Inc., New York, pp. 1–46.

Rastogi, S.C., Menne, T., Johansen, J.D., 2003. The composition of fine fragrances is changing. Contact Dermatitis 48, 130–132.

Sangwan, N., Farooqi, A., Shabih, F., Sangwan, R., 2001. Regulation of essential oil production in plants. Plant Growth Regul. 34, 3–21.

Simkin, A.J., Miettinen, K., Claudel, P., Burlat, V., Guirimand, G., Courdavault, V., Papon, N., Meyer, S., Godet, S., St-Pierre, B., 2012. Characterization of the plastidial geraniol synthase from *Madagascar periwinkle* which initiates the monoterpenoid branch of the alkaloid pathway in internal phloem associated parenchyma. Phytochem 85, 36–43.

Small, I., Peeters, N., Legeai, F., Lurin, C., 2004. Predotar: a tool for rapidly screening proteomes for N-terminal targeting sequences. Proteomics 4, 1581–1590.

Tarshis, L., Proteau, P.J., Kellogg, B.A., Sacchettini, J.C., Poulter, C.D., 1996. Regulation of product chain length by isoprenyl diphosphate synthases. Proc. Natl. Acad. Sci. USA 93, 15018.

Tholl, D., Lee, S., 2011. Elucidating the metabolism of plant terpene volatiles: alternative tools for engineering plant defenses. In: Gang, D.R. (Ed.), The Biological Activity of Phytochemicals. Springer Inc., Washington, pp. 159–178.

Thompson, J., Gibson, T., Plewniak, F., Jeanmougin, F., Higgins, D., 1997. The CLUSTAL_X windows interface: flexible strategies for multiple sequence alignment aided by quality analysis tools. Nucleic Acids Res. 25, 4876–4882.

Tikunov, Y., Lommen, A., De Vos, C., Verhoeven, H.A., Bino, R.J., Hall, R.D., Bovy, A.G., 2005. A novel approach for nontargeted data analysis for metabolomics. Large-scale profiling of tomato fruit volatiles. Plant Physiol. 139, 1125–1137.

Turner, G., Gershenzon, J., Nielson, E.E., Froehlich, J.E., Croteau, R., 1999. Limonene synthase, the enzyme responsible for monoterpene biosynthesis in peppermint, is localized to leucoplasts of oil gland secretory cells. Plant Physiol. 120, 879–886.

van der Hooft, J.J.J., Vervoort, J., Bino, R.J., de Vos, R.C.H, 2011. Spectral trees as a robust annotation tool in LC–MS based metabolomics. Metabolomics 8, 691–703.

van Engelen, F.A., Molthoff, J.W., Conner, A.J., Nap, J.P., Pereira, A., Stiekema, W.J., 1995. pBINPLUS: an improved plant transformation vector based on pBIN19. Transgenic Res. 4, 288–290.

van Herpen, T.W.J.M., Cankar, K., Nogueira, M., Bosch, D., Bouwmeester, H.J., Beekwilder, J., 2010. *Nicotiana benthamiana* as a production platform for *Artemisinin* precursors. PLoS One 5, e14222.

Voinnet, O., Rivas, S., Mestre, P., Baulcombe, D., 2003. An enhanced transient expression system in plants based on suppression of gene silencing by the p19 protein of tomato bushy stunt virus. Plant J. 33, 949–956.

Vom Endt, D., e Silva, M.S., Kijne, J.W., Pasquali, G., Memelink, J., 2007. Identification of a bipartite jasmonate-responsive promoter element in the *Catharanthus roseus* ORCA3 transcription factor gene that interacts specifically with AT-Hook DNA-binding proteins. Plant Physiol. 144, 1680–1689.

Wendt, K.U., Schulz, G.E., 1998. Isoprenoid biosynthesis: manifold chemistry catalyzed by similar enzymes. Structure 6, 127–133.

Wink, M., 2010. Introduction: biochemistry, physiology and ecological functions of secondary metabolites. In: Wink, M. (Ed.), Annual Plant Reviews: Biochemistry of Plant Secondary Metabolism, second ed. John Wiley & Sons, Inc., Oxford, UK, pp. 1–19.

Winterhalter, P., Skouroumounis, G., 1997. Glycoconjugated aroma compounds: occurrence, role and biotechnological transformation. Adv. Biochem. Eng. Biotechnol. 55, 73–105.

Wong, E.Y., Hironaka, C.M., Fischhoff, D.A., 1992. *Arabidopsis thaliana* small subunit leader and transit peptide enhance the expression of *Bacillus thuringiensis* proteins in transgenic plants. Plant Mol. Biol. 20, 81–93.

Yang, T., Li, J., Wang, H.X., Zeng, Y., 2005. A geraniol-synthase gene from *Cinnamomum tenuipilum*. Phytochem 66, 285–293.

Yang, T., Stoopen, G., Yalpani, N., Vervoort, J., De Vos, R., Voster, A., Verstappen, F.W.A., Bouwmeester, H.J., Jongsma, M.A., 2011. Metabolic engineering of geranic acid in maize to achieve fungal resistance is compromised by novel glycosylation patterns. Metab. Eng. 13, 414–425.